Ambipolar Electrical Transport in Semiconducting Single-Wall Carbon Nanotubes

R. Martel, V. Derycke, C. Lavoie, J. Appenzeller, K. K. Chan, J. Tersoff, and Ph. Avouris
IBM Research Division, T. J. Watson Research Center, Yorktown Heights, New York 10598
(Received 5 July 2001; published 3 December 2001)

Ambipolar electrical transport is reported in single-wall carbon nanotube (SWNT) field-effect transistors. In particular, the properties of SWNT junctions to TiC are discussed in detail. The carbide-nanotube junctions are abrupt and robust. In contrast to planar junctions, these contacts present low resistance for the injection of both p- and n-type carriers—the apparent barrier height of the junction is modified by the gate field. Thus SWNTs offer the novel possibility of ambipolar Ohmic contacts.

DOI: 10.1103/PhysRevLett.87.256805 PACS numbers: 85.35.Kt, 73.30.+y, 73.40.Sx, 73.63.Rt

Carbon nanotubes are quasi-one-dimensional molecular structures with semiconducting or metallic properties that make them promising material for future electronic applications [1]. One of the most interesting applications involves their use as channels of field-effect transistors [2,3]. The early nanotube devices were fabricated by depositing single-wall carbon nanotubes (SWNTs) on top of high work function ($\phi > 5$ eV) metal electrodes such as platinum or gold. These devices had generally high contact resistances. More importantly, they were invariably unipolar with p-type characteristics (hole transport) [4]. The origin of the p-type character of semiconducting SWNTs (s-SWNTs) remains an open question. Several proposals have been made to explain this effect, including contact doping [2,5], doping introduced by cleaning and handling the nanotubes in oxidizing acids [3], or doping by the adsorption of atmospheric oxygen [6–8]. In principle, any of the above mechanisms can influence the transistor characteristics.

This Letter presents the properties of "end-bonded" nanotube-metal contacts and their influence on the nanotube transistor characteristics. In particular, the characteristics of carbon nanotube field-effect transistors (CNFETs) made of s-SWNTs contacted to titanium carbide (TiC) and passivated with a uniform SiO_2 layer are presented in detail. In contrast to planar devices, here the apparent barrier height for carrier injection is modulated by the gate field, allowing CNFETs to be ambipolar with low contact resistance for both n- and p-type conduction. Furthermore, we find that the usual p-type character of CNFETs is not an intrinsic property of the nanotube, but rather appears to be a property of the nanotube-metal junction.

Carbides are known to be formed at the interface between a graphite layer and a metal [9]. Carbide formation by multiwall carbon nanotubes (MWNTs) and SWNTs has been reported recently by Zhang *et al.* at temperatures above 950 °C [10]. Titanium carbide contacts involving MWNTs show low resistance [10,11], presumably because of the direct electrical contact of the metal with several layers of the nanotube.

Here we present a study of nanotube-carbide interface formation and its use in making SWNT FETs. Carbide contacted CNFETs were fabricated from a large array of devices made of 1.4 nm diameter s-SWNTs (band gap $E_g \approx 600$ meV) dispersed on a SiO_2 layer (150 nm thick) over a p^+ Si substrate [12]. Titanium contacts (50 nm thick) were formed using optical lithography and standard lift-off techniques. The carbide formation was then monitored by time resolved x-ray diffraction (XRD) with 0.180 nm synchrotron radiation [13]. Figure 1a presents rapid XRD data acquired *in situ* from a small section of the substrate as a function of annealing temperature (3 °C/s ramp) in helium. Below 700 °C, a very intense XRD peak just below $2\theta \approx 44°$ corresponding to the $\langle 0002 \rangle$ diffraction line of the hexagonal phase of the titanium film dominates the signal. A first transformation is clearly observed just above 700 °C to form a titanium carbide (Ti_xC) phase with diffraction peaks at $2\theta \approx 41°$ and $\approx 50°$. Above

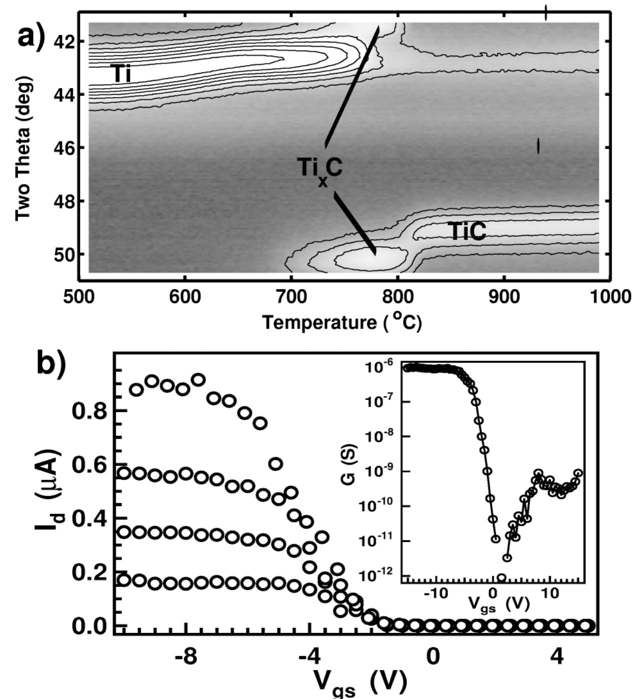

FIG. 1. (a) Evolution of the x-ray diffraction of a titanium film (50 nm) covering SWNTs dispersed on a SiO_2/Si substrate as a function of temperature. (b) Transfer characteristics of an 800 nm CNFET taken at V_{ds} from 0.2 to 0.8 V in 0.2 V steps. Inset: conductance at $V_{ds} = 0.8$ V as a function of V_{gs}.

 0031-9007/01/87(25)/256805(4)$15.00 © 2001 The American Physical Society

800 °C, one sees the transformation of the former phase and the appearance of two new intense XRD peaks. The intensity of the peaks stays constant up to 1100 °C. This reaction is the formation of the cubic TiC phase. The XRD peaks of this phase are detected at $2\theta \approx 49°$ and 43°, which correspond, respectively, to the $\langle 200 \rangle$ and the $\langle 111 \rangle$ plane of the TiC crystal [14].

Several CNFETs were prepared by quenching the substrate at the temperature of the TiC phase transformation (800–850 °C). The devices were then protected with a 10 nm SiO_2 layer deposited at room temperature and densified by annealing at 400 °C for 30 min in forming gas. The conductance for hole transport (negative V_{gs}) measured after the carbide reaction improved by more than 2 orders of magnitude in several of the individual nanotube devices. Moreover, the CNFETs involving small bundles of SWNTs now show significant conductance in the "OFF" state, indicating that metallic SWNTs in the core of the ropes have also been contacted. These results confirm electrically the reaction and the penetration of the Ti metal to form nanotube-TiC crystal junctions. Using transmission electron microscopy (TEM), we examined cross sections of the substrate (not shown). The TEM images confirm that the Ti atoms have diffused to the core of the rope and formed a TiC crystal. The nanotubes in the bundles are end bonded to the TiC crystal and the interface is *abrupt.*

As an example, the transfer characteristics of an 800 nm long (~1.4 nm diameter) CNFET [15] prepared by this method are presented in Fig. 1b. The transistor is p-type and its transconductance (dI_d/dV_g) is 2×10^{-7} A/V. Most of the devices prepared show drastic improvement of the transconductance, which before carbide formation was $\approx 10^{-9}$ A/V. Overall, the device characteristics were improved, with the gate modulating the conductance by about 6 orders of magnitude (Fig. 1b inset). CNFETs have low conductance at $V_{gs} = 0$ V, consistent with a low dopant concentration in the nanotube [16].

Some of the carbide devices show weak evidence of electron transport in the inversion region, i.e., at $V_{gs} > 0$ V (see Fig. 1b inset). Further annealing at 700 °C (30 sec) in argon removes adsorbed atmospheric gases by thermal desorption through the thin SiO_2 layer. This treatment increases the conductance at positive V_{gs} of all the CNFETs, as shown in the sequence in Fig. 2. On the other hand, similar annealing without the SiO_2 layer produced only unipolar p-type devices (no current at positive V_{gs}). The electrical transport in the CNFETs passivated with SiO_2 becomes fully ambipolar after another annealing at 800 °C. The new conduction channel involves electrons and appears without a significant change of the conductance at negative V_{gs} (see example in Fig. 2). The ambipolar device is stable in air.

Surprisingly, these devices show Ohmic I-V_{ds} curves in both the strong accumulation (holes) and inversion (more precisely, electron accumulation) regimes. This suggests that the Schottky barriers at the contact are very small for both electron and hole transport. Normally, the sum of

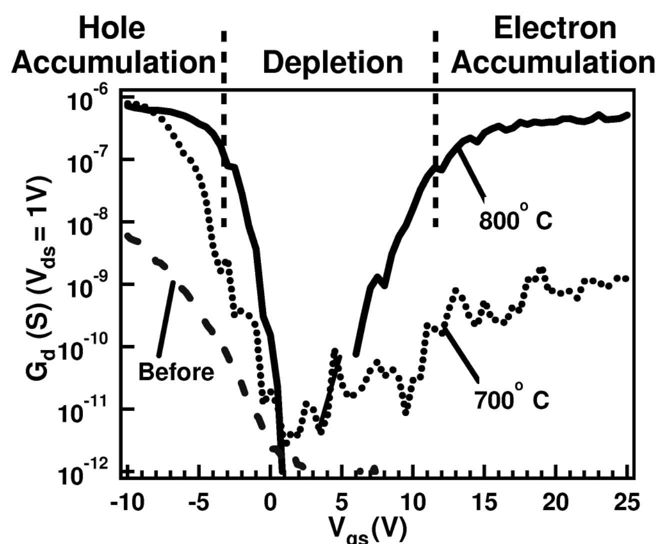

FIG. 2. Transfer characteristics in conductance unit (G_d) of an 800 nm CNFET at different processing stages. The dashed line shows the characteristics of the device after a mild anneal at 300 °C. The dotted line is obtained after the formation of the TiC contacts (see text) and an additional anneal to 700 °C for 30 sec with a covering SiO_2 layer (10 nm). The full line is obtained after another anneal at 800 °C for 30 sec.

the barrier heights for electrons and holes is expected to equal the band gap. We therefore explore in detail the properties of these barriers as a function of temperature and bias conditions.

Figure 3 presents the results measured on a 1.5 μm long CNFET. The barriers for electron and hole injection are measured from a large number of I-V_{ds} curves taken from 4 to 300 K, with $V_{gs} = -13$ and 18.7 V, i.e., in the strong hole and electron accumulation regions, respectively. Figure 3a shows a set of these curves in the hole transport region and an Arrhenius plot of the current (inset) from which the thermionic and tunneling contributions can be identified. Similar results were obtained for electron transport and the data are qualitatively the same. At 4 K there is no detectable current (using either ac or dc methods) for V_{ds} below $\approx$10 meV at any V_{gs} between -25 and 25 V. This is consistent with the presence of a small Schottky barrier. The tunneling current dominates at the lowest temperatures for $|V_{ds}| > 10$ meV. A clear thermionic regime is observed in both electron and hole transport at temperatures above $T = 25$ K (Fig. 3a inset). As shown in Fig. 3b, the barrier heights at zero field (ϕ_o) for electron and hole injection are 13 and 15 meV, respectively. The roughly symmetrical barriers suggest that E_F at the junction lines up close to the middle of the gap of the s-SWNT. Yet these values are about 20 times smaller than the expected barriers for a Fermi level pinned in the middle of the band gap of the s-SWNT (i.e., $\phi_b \sim E_g/2 = 300$ meV).

The possibility that the observed transport behavior arises from a single SWNT with a small band gap [17] can be ruled out because the conductance at room temperature is essentially zero when the device is in the

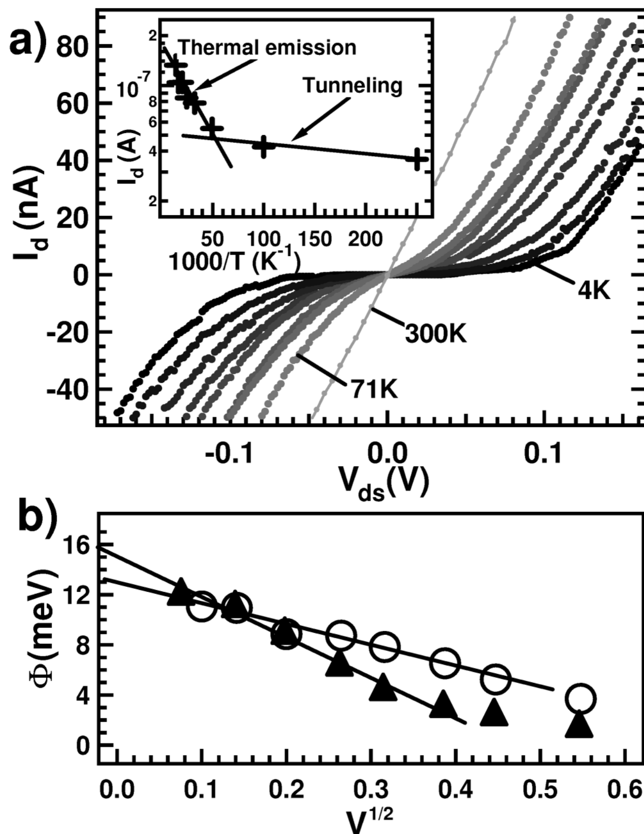

FIG. 3. Characterization of the barriers for electron and hole injection into a 1500 nm long CNFET. (a) I-V_{ds} curves taken at $V_{\mathrm{gs}} = -13$ V for different temperatures (4, 10, 20, 39, 41, 49, 69, and 71 K). Inset: Arrhenius plot for hole transport at $V_{\mathrm{ds}} = 150$ mV. (b) Plot of the barrier height for electrons (open circles) and holes (dark triangles) as a function of the square root of V_{ds}. The barrier height in the absence of the field is extrapolated at $V_{\mathrm{ds}} = 0$.

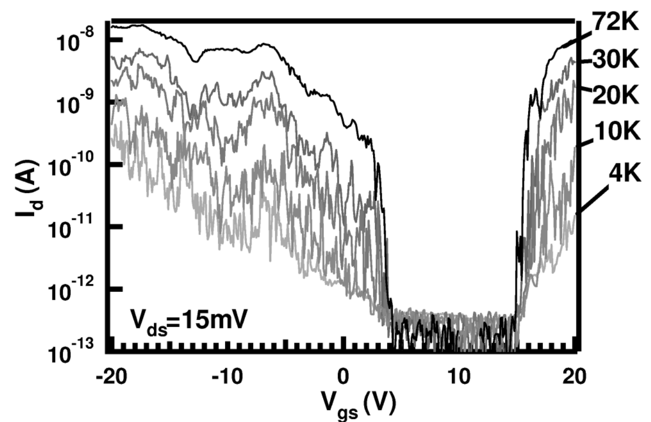

FIG. 4. Transfer characteristics of the CNFET (Fig. 3) at $V_{\mathrm{ds}} = 15$ meV as a function of temperature.

OFF state. It is also unlikely that the behavior results from two independent s-SWNTs doped p- and n-type, coexisting in the small SWNT bundle. Devices made with small bundles of s-SWNTs or individual s-SWNT show a continuous transformation from p-type to ambipolar CNFETs (see an example in Fig. 2). The presence of a mixture can also be ruled out from selective breakdown experiments at large negative V_{gs} [18]. The breakdown of the s-SWNTs under these conditions should destroy only the n-type tube and leave the p-type one unaffected, which is, however, not the case. Finally, although most of the semiconducting tubes present an ≈600 meV band gap [5], the vast majority of CNFETs fabricated are ambipolar.

We can therefore conclude that, contrary to all expectations, the contacts have only very small barriers for both electrons and holes. The effect of this on the device transfer characteristics is illustrated in Fig. 4. The characteristics taken with a small V_{ds} value as a function of the temperature clearly confirm that the contact barrier is small in both the hole and electron accumulation regimes. The current increases with temperature because of a thermionic emission over this barrier. This effect introduces a drastic change of the shape of the I_d vs V_{gs} curves in the threshold regions. Above 70 K, the switching is very abrupt, and the I_d vs V_{ds} curves measured for both electron and hole transport become truly Ohmic near 300 K, as in Fig. 3a.

The low barriers for both electrons and holes indicate that the effective barrier heights are strongly modulated by the electrostatic field of the gate. This is not possible in familiar planar devices. The electronic behavior of nanotube contacts is uniquely sensitive to the electrostatics [19], because of their quasi-one-dimensional structure. Fermi-level pinning, which dominates the behavior of planar contacts, becomes relatively unimportant for nanotubes [19]. Moreover, the metallic carbide contact tends to form a needlelike shape [10] which can focus the electric field. Thus the gate can induce a stronger electric field at this junction than at a planar contact. As illustrated in Fig. 5, the result can be a "true" Schottky barrier height, ϕ_b, that is as large as expected, but so thin that carriers can easily tunnel through the barrier. Similarly, we observed ambipolar transport in all of the side-bonded nanotube-metal junctions tested so far after an anneal to 500 °C in vacuum (Au, Ti, and Co). Although the shape of the contact region is less clear in those cases, the central feature in these junctions is clearly related to their 1D structure. Therefore, we speculate that field focusing occurs in these junctions as well.

Ohmic tunneling barriers can be achieved for planar contacts only by strong chemical doping. We believe that it is the unique geometry of nanotube contacts that permits such Ohmic tunneling contacts to be induced by the gate field alone. In this picture, the small apparent barrier height, ϕ_o, in Fig. 3 arises because, for electrons (or holes) near the Fermi level, the tail of the barrier is too wide to tunnel through (see Figs. 5a and 5b). Only at slightly higher energy is the barrier sufficiently thin for tunneling, so the carriers must be thermally excited above the wide part of the barrier. Tunneling is particularly important in s-SWNT contacts because the midgap tunneling length [19] is roughly 3 times as long as in silicon.

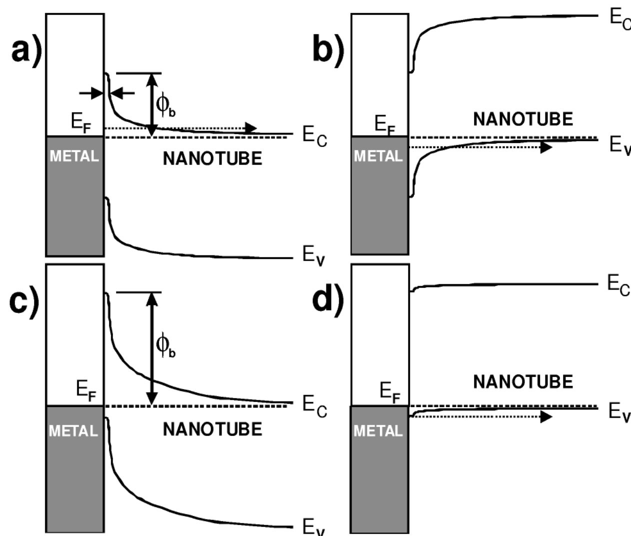

FIG. 5. Schematics of the bands along the length of the nanotube at different electrostatic gate fields. (a) and (b) show the barriers for the ambipolar device in the strong electron ($V_{gs} \gg 0$) and hole ($V_{gs} \ll 0$) accumulation regions, respectively. (c) and (d) illustrate the situation in the presence of oxygen for the electron and hole accumulation regions, respectively. The barrier is thin for injection at high excess energy (arrows). The dotted arrows show the injection of carriers at $E \sim k_B T$.

Near the interface, the position of the Fermi level within the s-SWNT band gap is expected to obey the Schottky work function rule, with only a localized perturbation from interface states [19,20]. An adsorbed gas can alter the work function or introduce a dipole near the junction. We speculate that this is the origin of the p-type behavior in air. Figures 5c and 5d show the situation when the metal work function is increased, as by adsorbed oxygen. In this case, it is easy to have an Ohmic contact for holes at negative gate voltage. However, for positive gate voltage, the same gate field is no longer sufficient to give a low barrier for electrons. Thus the usual p-type behavior could be due to a high barrier at the contacts, rather than fixed carrier type along the length of the tube. The role of gas on the contact barrier will be discussed in detail elsewhere [21].

In conclusion, the ambipolar CNFETs work in both the hole and electron accumulation regimes with comparable performance. As a result, they can be exploited to implement complementary logic [21]. The possibility of ambipolar Ohmic contacts illustrates the unique opportunities offered by carbon nanotube devices.

The authors thank P.-H. Wong for his support and for valuable discussions, also F. Leonard for useful discussions, B. Ek, L. Gignac, and P. G. Collins for technical assistance, and Cyril Cabral, Jr. and Jean Jordan-Sweet for support with the synchrotron XRD experiments.

[1] *Carbon Nanotubes: Synthesis, Structure, Properties, and Applications,* edited by M. Dresselhaus, G. Dresselhaus, and Ph. Avouris (Springer-Verlag, Berlin, 2001).
[2] S. J. Tans, A. R. M. Verschueren, and C. Dekker, Nature (London) **393**, 49 (1998).
[3] R. Martel, T. Schmidt, H. R. Shea, T. Hertel, and Ph. Avouris, Appl. Phys. Lett. **73**, 2447 (1998).
[4] Weak signature of n-type transport has been observed recently by C. Zhou, J. Kong, and H. Dai, Appl. Phys. Lett. **76**, 1597 (2000); J. Park and P. L. McEuen, Appl. Phys. Lett. **79**, 1363 (2001).
[5] J. W. G. Wildoer *et al.,* Nature (London) **59**, 391 (1998).
[6] P. G. Collins *et al.,* Science **287**, 1804 (2000).
[7] J. Kong *et al.,* Science **287**, 622 (2000).
[8] G. U. Sumanasekera, C. K. W. Adu, S. Fang, and P. C. Eklund, Phys. Rev. Lett. **85**, 1096 (2000).
[9] J. Roth, H. Graupner, S. P. Withrow, D. Zehner, and R. A. Zuhr, J. Appl. Phys. **79**, 7695 (1996).
[10] Y. Zhang, T. Ichihashi, E. Landree, F. Nihey, and S. Iijima, Science **285**, 1719 (1999).
[11] J.-O. Lee, C. Park, J.-J. Kim, J. Kim, J. W. Park, and K.-H. Yoo, J. Phys. D **33**, 1953 (2000).
[12] The SWNTs were prepared by laser ablation as described by A. Thess *et al.,* Science **273**, 483 (1996). They were used without further treatment and dispersed in dichloroethane by a short exposure to ultrasound.
[13] The experiments were performed using the IBM/MIT beam line X20C located at the National Synchrotron Light Source in Brookhaven National Laboratory under DOE Contract No. DE-AC02-76CH-00016. See a description by C. Lavoie *et al.,* Mater. Res. Soc. Symp. Proc. **406**, 163 (1996).
[14] Handbook for diffraction data, (PCPDFWIN ver. 2.00) JCPDS 1998.
[15] The diameter of the nanotube channel is measured using the apparent height from an atomic force microscope (AFM) image. In principle, the channel is composed of a single SWNT or a bundle of a few SWNTs [see S. S. Wong *et al.,* Appl. Phys. Lett. **73**, 3465 (1998)].
[16] We paid special attention to avoid unintentional doping through oxidative purification of the tubes [see Z. Yu and L. Brus, J. Phys. Chem. B **104**, 10 995 (2000)].
[17] C. Zhou, J. Kong, and H. Dai, Phys. Rev. Lett. **84**, 5604 (2000).
[18] P. G. Collins, M. R. Arnold, and Ph. Avouris, Science **292**, 706 (2001).
[19] F. Leonard and J. Tersoff, Phys. Rev. Lett. **84**, 4693 (2000).
[20] A. Rochefort, M. DiVentra, and Ph. Avouris, Appl. Phys. Lett. **78**, 2521 (2001).
[21] V. Derycke *et al.,* Nano Letters **1**, 453 (2001); V. Derycke *et al.* (to be published).